



저작자표시 2.0 대한민국

이용자는 아래의 조건을 따르는 경우에 한하여 자유롭게

- 이 저작물을 복제, 배포, 전송, 전시, 공연 및 방송할 수 있습니다.
- 이차적 저작물을 작성할 수 있습니다.
- 이 저작물을 영리 목적으로 이용할 수 있습니다.

다음과 같은 조건을 따라야 합니다:



저작자표시. 귀하는 원저작자를 표시하여야 합니다.

- 귀하는, 이 저작물의 재이용이나 배포의 경우, 이 저작물에 적용된 이용허락조건을 명확하게 나타내어야 합니다.
- 저작권자로부터 별도의 허가를 받으면 이러한 조건들은 적용되지 않습니다.

저작권법에 따른 이용자의 권리는 위의 내용에 의하여 영향을 받지 않습니다.

이것은 [이용허락규약\(Legal Code\)](#)을 이해하기 쉽게 요약한 것입니다.

[Disclaimer](#) 

Master's Thesis
석사 학위논문

**First Principles Study of Morphology, Doping Level and
Water Solvation Effects on Catalytic Mechanism of a
Graphene Towards Oxygen Reduction Reaction**

Dohyun Kwak (곽도현 郭棹現)

Department of Energy Systems Engineering
에너지시스템공학전공

DGIST

2015

First Principles Study of Morphology, Doping Level and Water Solvation Effects on Catalytic Mechanism of a Graphene Towards Oxygen Reduction Reaction

Advisor: Professor Byungchan Han

Co-advisor: Doctor Young-Gi Yoon

by

Dohyun Kwak

Department of Energy Systems Engineering

DGIST

A thesis submitted to the faculty of DGIST in partial fulfillment of the requirements for the degree of Master of Science in the Department of Energy Systems Engineering. The study was conducted in accordance with Code of Research Ethics¹⁾

12. 3. 2014

Approved by

Professor Byungchan Han
(Advisor)

Doctor Young-Gi Yoon
(Co-Advisor)

¹⁾ Declaration of Ethical Conduct in Research: I, as a graduate student of DGIST, hereby declare that I have not committed any acts that may damage the credibility of my research. These include, but are not limited to: falsification, thesis written by someone else, distortion of research findings or plagiarism. I affirm that my thesis contains honest conclusions based on my own careful research under the guidance of my thesis advisor.

First Principles Study of Morphology, Doping Level and Water Solvation Effects on Catalytic Mechanism of a Graphene Towards Oxygen Reduction Reaction

Dohyun Kwak

Accepted in partial fulfillment of the requirements for the degree of Master of
Science

12. 3. 2014

Head of Committee _____(인)

Prof. Byungchan Han

Committee Member _____(인)

Dr. Young-Gi Yoon

Committee Member _____(인)

Prof. Sangaraju Shanmugam

MS/ES

곽도현. Dohyun Kwak. First Principles Study of Morphology, Doping Level and Water

Solvation Effects on Catalytic Mechanism of a Graphene Towards Oxygen Reduction

201324001

Reaction. Department of energy Systems Engineering. 2014. 28 p. Advisors Prof.

Byungchan Han, Doctor Co-Advisors Young-Gi Yoon

Abstract

First principles density functional theory calculations are utilized to unveil oxygen reduction reaction mechanisms on nitrogen doped graphene (N-Gr). Considering the effect of both the geometry and concentration of N in bulk and edge N-Gr forms, we calculate the energies of a large number of model systems to cover a wide range of possible N-Gr structures and determine the most stable ones. In agreement with experiments, our calculations suggest that doping levels in stable N-Gr forms are limited to less than about 30 at.%, above which the hexagonal graphene framework is broken. Remarkably, the ground state structures of bulk and edge N-Gr are found to differ depending on the doping level and poisoning of the edge bonds. ORR mechanisms are estimated using Gibbs free energy diagrams, both with and without water solvation. Our results indicate that N doping significantly alters the catalytic properties of pure graphene and that dilutely doped bulk N-Gr forms are the most active.

Keywords: First principles, Renewable energy, Graphene, Catalyst, Oxygen reduction reaction

Contents

Abstract	I
Contents	II
List of Figures	III
1. Introduction	1
1.1. Introduction to First principles DFT calculations	1
1.2. Background	1
2. Methodology and Model Systems	3
2.1. Computational Details.....	3
2.2. DFT calculations of stable N-Gr Structures	4
2.3. Poisoning of dangling bonds in edge N-Gr.....	6
3. Results and Discussion	11
3.1. Electronic structures of N-Gr model systems	11
3.2. Thermodynamic free energy diagram of ORR: Formalism	12
3.3. Gibbs free energy diagrams for ORR: The effect of dopant concentration	13
3.4. Thermodynamic free energy diagram of ORR: Effect of water solvation	18
4. Conclusion	20
References	21
Summary(국문요약)	25
Acknowledgement	26
Curriculum Vitae	27

List of Figures

- Figure 1. DFT calculated energy convex hull of 752 bulk N-doped graphene structures as a function of the doping level and arrangement of N and C atoms. Each N atom substitutes a C atom in (3×3) graphene sheets. The blue circles on the convex hull represent ground state structures at that given at.% N. 4
- Figure 2. DFT calculated energy convex hull of 110 edge N-doped graphene model systems as a function of the doping level and relative arrangement of N and C atoms. The blue circles represent ground state structures that together form the energy convex hull as in Fig. 1. 4
- Figure 3. Schematic diagrams explaining the chain of reactions leading to the thermodynamically most stable configurations of edge N-Gr at (a) 5.5 at.% N, (b) 16.7 at.% N and (c) 27.8 at.% N. Each of the model systems was rigorously evaluated for adsorption by solvated protons and O₂ molecules. The reversible potentials for the electrochemical steps were identified using Eq. (2)..... 8
- Figure 4. Model bulk and edge N-Gr systems are used in this study to investigate fundamental mechanisms of ORR catalysis. The dashed parallelograms denote the unit cells used in DFT calculations..... 10
- Figure 5. Charge density distribution calculated by Bader's analysis for (a) 5.5 at.% N bulk and in (b) 5.5 at.% N edge N-Gr models..... 12
- Figure 6. (a) Free energy diagrams of ORR on edge and bulk N-Gr models at potential $U = 1.23$ V. Free energy diagrams of ORR at thermodynamic onset potentials on bulk N-Gr models (b) and edge N-Gr models (c). Here, the effect of water solvation was not considered, and the solid lines represent potential determining step..... 15
- Figure 7. A proposed ORR pathway for the edged form of N-Gr with 27.8 at.% N-doping level. Detailed catalysis cycle for ORR of the edged form of N-Gr was illustrated via a series of electrochemical reaction steps. 17
- Figure 8. (a) Free energy diagrams of ORR on edge and bulk N-Gr models at potential $U = 1.23$ V. Free energy diagrams of ORR at thermodynamic onset potentials on bulk N-Gr models (b) and edge N-Gr models (c). Here, the effect of water solvation was considered, and the solid lines represent potential determining step..... 19

1. Introduction

1.1. Introduction to First principles DFT calculations

Various computational methods have been developed to investigate material properties and design new material over half century. Most computational methods use any empirical parameters or assumptions for matching experimental results, while first-principles calculations directly obtain the material properties without any empirical parameters by solving the Schrödinger equations. First principles calculations, however, require considerable amounts of computational resources to calculate a large number of interactions between electrons of atoms. Kohn and Sham developed the density functional theory (DFT) to simplify the interactions between electrons of atoms by using a unique functional of the electron density. Thus, DFT methods reduce the variables of wave function from $3N$ (number of electrons) to only 3 coordinates and the calculation time to investigate material properties. First principles DFT calculations provide ground state energy, charge density, and band structure, which relate to the quantitative material properties. In this thesis, oxygen reduction reactions of nitrogen doped graphene were studied by using the first principles DFT calculations.

1.2. Background

Securing renewable energy sources is one of the most urgent challenges of our century. Fossil fuels are a limited resource and their use often has serious environmental impacts. As a result there has been a major drive recently to advance science and technology for harvesting green and renewable energies using, for instance the chemical energies of hydrogen and oxygen, photons, or biomass, Well to device energy conversion efficiencies of current processes in these fields, however, are still too low to be utilized for any practical-scale purpose and are often hampered by imperfect catalyst materials.

Efficiency of reducing oxygen plays a key role in controlling over all performances of energy systems in many industrial sectors, for instance, fuel generation devices,[1, 2] metal-air batteries,[3-5] and fuel cells[6-8] etc. One of the best examples is the Proton Exchange Membrane (PEM) fuel cell. In spite of its highly expected and theoretically possible high thermodynamic efficiency and environmentally friendly nature, ORR catalysts in the system still depend on pure or alloys of Pt, which is quite expensive and provides efficiencies that are not high

enough to compete with conventional fossil fuel energy systems.

Doping pure substances with heteroatoms, by even very small amounts, often gives rise to material properties that are very different from those of the parent materials. This approach has been widely applied for devices such as semi-conductors, sensors and energy systems.[9-13]

Graphene doped with nitrogen atoms, or N-Gr, is considered a very promising material for replacing the costly Pt based metallic catalysts, since it has been discovered to show a markedly increased ORR activity as compared to pristine graphene.[14-16] In addition, N-Gr has been found to be much more stable against peroxides and takes part in the ORR reaction via a four-electron process, ultimately yielding water.[15-17] This implies that doping can completely modify the electronic structure or ORR mechanism of pristine graphene, which was confirmed in a study by Qu et al.,[16] who reported that pure graphene showed a two-step, two-electron process for oxygen reduction with low onset potential (-0.45 V and -0.7 V vs Ag/AgCl), while N-Gr exhibited a four-electron pathway with activity three times higher than Pt/C in alkaline media.

However, the oxygen reduction reaction (ORR) mechanisms in N-Gr are not clearly understood, as manifested in the widely scattered and inconclusive data consisting of both experimental measurements and theoretical calculations. For example, experimentally measured and calculated onset potentials for ORR in N-Gr have been reported in the range of 0.5 ~ 0.9 V (vs. NHE).[15-22] Moreover, there are a variety of theoretical studies for ORR mechanisms, and it was proposed that ORR activity on graphene-based-catalysts should be comparable to the state-of-the-art Pt catalyst.[23, 24] Kim et al.[25] proposed that the morphology of N-Gr (i.e., edge or bulk) is vital for controlling ORR activity, while Okamoto[26] has argued that the concentration of dopant N atoms around the C atom is the key to understanding ORR. Independent of the arguments based on structure, it has also been suggested that the activity could be attributed to delocalization of electronic charge in the C atoms neighbouring the dopant N atom.[27, 28] These properties of N-Gr make it especially attractive as an option for replacing costly Pt-based metallic catalysts in PEM Fuel cells.[17]

Development of highly functional doped N-Gr requires an accurate understanding of the underlying mechanisms using well-defined model systems and fundamental tools. To accomplish this goal, we utilize first principles density functional theory (DFT) calculations to bulk and edged forms of N-Gr, with varying N doping level. By rigorously screening approximately 900 N-Gr model systems, we will first identify the thermodynamically

favoured ground state structures. Furthermore, we will evaluate the onset potentials for ORR on each of the structures by calculating the thermodynamic free energy diagrams and by taking into account the explicit effect of solvation due to water.

2. Methodology and Model Systems

2.1. Computational Details

The model system for pure graphene was set up with a single layer of (3×3) hexagonal graphene framework. Then the dopant N atoms were allowed to substitute the C atoms to make N-Gr sheets. All energy calculations in our models were performed using VASP.[29, 30] Projector Augmented Wave (PAW) pseudo-potentials[31] as implemented in VASP were used for describing the interactions between ions and electrons, and the exchange-correlation energy of electrons was described by employing the generalized gradient approximation (GGA) using the Perdew-Burke-Ernzerhof (PBE) functionals.[32] Van der Waals (vdW) corrections were performed using the Grimme scheme.[33] The Kohn-Sham orbitals were expanded on a plane wave basis set with a cutoff energy of 520 eV. All atoms were fully relaxed until the sum of forces was less than 10^{-4} eV/Å. To integrate the Brillouin zone, a gamma point mesh with $5\times 5\times 1$ k-points was used and periodic boundary conditions were imposed on the N-Gr models with a large vacuum space of 14 Å in the direction perpendicular to graphene surface for the bulk and edge N-Gr forms. An additional 11 Å were added in the direction perpendicular to the edge but in the same plane for the edged sheets to preclude interactions with images.

2.2. DFT calculations of stable N-Gr Structures

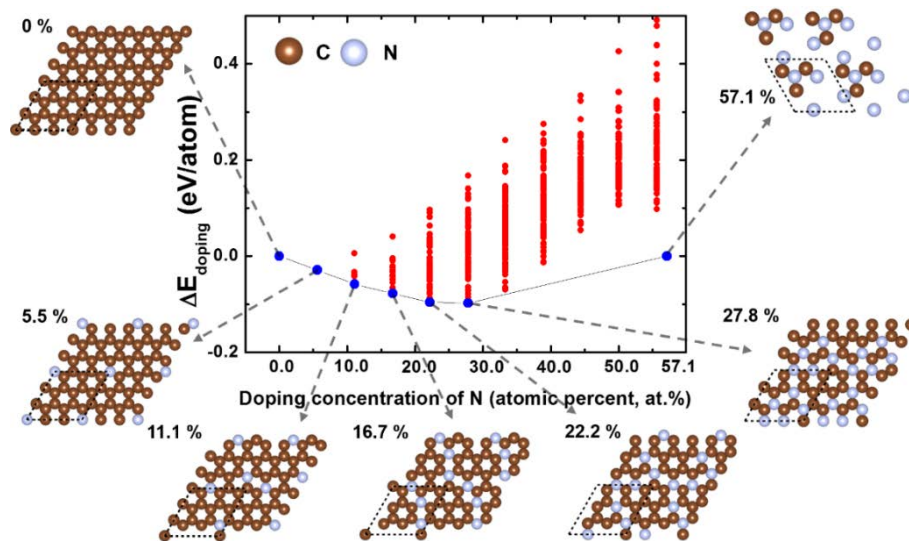


Figure 1. DFT calculated energy convex hull of 752 bulk N-doped graphene structures as a function of the doping level and arrangement of N and C atoms. Each N atom substitutes a C atom in (3×3) graphene sheets. The blue circles on the convex hull represent ground state structures at that given at.% N.

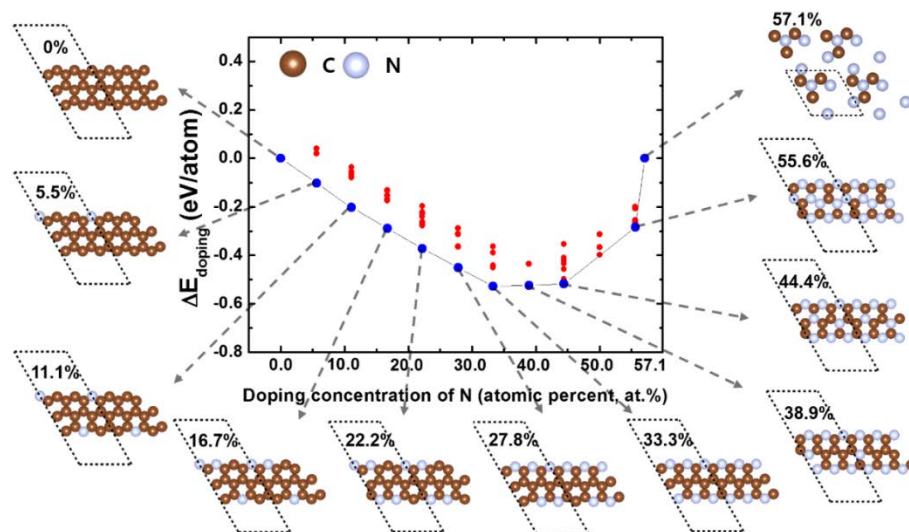


Figure 2. DFT calculated energy convex hull of 110 edge N-doped graphene model systems as a function of the doping level and relative arrangement of N and C atoms. The blue circles represent ground state structures that together form the energy convex hull as in Fig. 1.

Using first principles DFT calculations for the ground state energy, we screened 752 bulk and 110 edge shapes of N-Gr as function of the dopant concentration and substitutional configuration. The numerous model systems were generated by employing computer programs based on the cluster expansion theory.[34] In such an approach, it is possible to have several structures having the same at.% N due to different relative arrangements of C and N atoms. The most stable structures at a given at.% N can be readily identified from the thermodynamic energy convex hull, which indicates the thermodynamically most plausible phase transition path among the calculated structures in the process of doping, as shown in Fig. 1 for bulk and in Fig. 2 for edge N-Gr.

The doping energy at an atomic percentage (at. %) of θ , $\Delta E_{\text{doping}}(\theta)$, of each N-Gr structure is defined as given in Eq. (1),

$$\Delta E_{\text{doping}}(\theta) = E(\theta) - \left\{ \left(E(\theta_{\text{max}}) - E(\theta_{\text{min}}) \right) \frac{\theta - \theta_{\text{min}}}{\theta_{\text{max}} - \theta_{\text{min}}} + E(\theta_{\text{min}}) \right\} \quad (1).$$

Here, θ is the at.% of a doped N with the corresponding values of θ_{min} and θ_{max} being 0 and 57.1 at. % N respectively. $E(\theta)$ is the DFT-calculated total energy for total energy for an N-Gr structure at θ . $E(\theta_{\text{min}})$ and $E(\theta_{\text{max}})$ are DFT-calculated energies for pristine graphene and carbon nitride ($\beta\text{-C}_3\text{N}_4$), and are used as reference models.[35] N-Gr with $\theta = 100$ at.% N was not used as a reference because no such form has been reported in the literature until now. The doping energy ΔE_{doping} implies an amount of relative stabilization with respect to the hypothetical straight line connecting the energy levels of the two reference model systems. Understandably, the lower (more negative) is the doping energy at a given θ (or x), the higher is its relative stability.

Bulk N-Gr (graphitic N type) materials with θ below ~ 10 at.% N have been found in many experimental studies,[15-19] while higher θ are rarely reported. Souto et al.[36] have found that N-Gr materials with $\theta \leq 20$ at.% N maintain a graphite-like structure, and above this value they transform into the $\beta\text{-C}_3\text{N}_4$ phase due to the repulsive interaction between the lone-pairs in doped N. Our findings agree well with these observations as shown in Fig. 1, where N-Gr structures with 5.5, 11.1, 16.7, 22.2, and 27.8 at.% N can be seen to be thermodynamically stable. In Fig. 1, one can also clearly observe a two-phase equilibrium region from 27.8 to 57.1 at.% N, implying that

structures in this region are thermodynamically unstable against decomposition into two N-Gr configurations with 27.8 and 57.1 at.% N. Relative amounts of the decomposed structures can be determined thermodynamically using the lever-rule. We found that the metastable hexagonal framework of the graphene sheet was destroyed due to strong repulsions between N atoms in this range of at.% N. Thus, the material no longer retains its original properties. These findings imply that thermodynamically, a doping level of ≤ 30 at.% N is feasible on graphene, above which the specific advantages of N-Gr as an ORR catalyst may disappear.

Fig. 2 illustrates a similar DFT calculated energy convex hull for the edge forms of N-Gr, where we plot the doping energy as defined in Eq.1. Our results show that N-Gr structures with doping levels of 5.5, 11.1, 16.7, 22.2, 27.8, 33.3, 38.9, 44.4 and 55.6 at.% N are energetically stable. Above the 55.6 at.% N, however, the hexagonal framework of an edged N-Gr is broken due to strong repulsion between the lone pair electrons of the dopant N.

On comparing the magnitude of the doping energy, the edge N-Gr models can be predicted to be able to accommodate higher N atoms than the bulk form. We propose that the reason for stability at relatively higher at.% N in edge N-Gr is at easier release of strain energy owing to the location of N atoms at undercoordinated sites, which is not facilitated in bulk form. Doped N atoms form a zigzag topology in edge N-Gr, which helps in overcoming the electrostatic repulsion between lone pairs from neighbouring N atoms. Predictably, one can assert that the experimental synthesis of edge N-Gr should be easier than the bulk form with increasing at.% N. This assertion is in excellent agreement with experimental results.[15, 21, 25]

2.3. Poisoning of dangling bonds in edge N-Gr

Before investigating ORR mechanisms in edge N-Gr model systems captured by the energy convex hull, as shown in Fig. 2, we further thermodynamically studied whether atoms located at the edge boundaries (C and N), which have dangling bonds, are poisoned by the first ORR process. Specifically, we considered the electrochemical reaction of each the model systems with 5.5, 16.7 and 27.8 at.% N in edge N-Gr with ($\text{H}^+ + \text{e}^-$), and calculated the reversible potentials at $T = 300$ K, $P = 1$ atm and $\text{pH} = 0$. The reversible potentials were calculated using Eq. (2) as:

$$U_{\text{rev}} = -\Delta G_{\text{ads}} / nF \quad (2).$$

where U_{rev} and ΔG_{ads} are the reversible potential of the electrochemical reaction and change of Gibbs free energy during adsorption of H at the edge site, respectively. F is the Faraday constant and n is the number of electrons involved in the electrochemical reaction (here, $n = 1$). The change in zero point energy and entropy corrections were included in the Gibbs free energy change, as described in earlier studies.[37]

The first schematic, as shown in Fig. 3(a), demonstrates how N and C atoms, located on the boundary in edge N-Gr with 5.5 at.% N, can form strong chemical bonds with H atoms at potentials below 0.86 V (vs SHE). Considering the fact that typical operational potentials of PEM fuel cells are below 0.8 ~ 0.9 V (vs SHE), H atoms poison all N atoms in edge N-Gr with 5.5 at.% N. Poisoning of these dangling bonds by either O or O₂ was not found to be thermodynamically more favourable than by H.

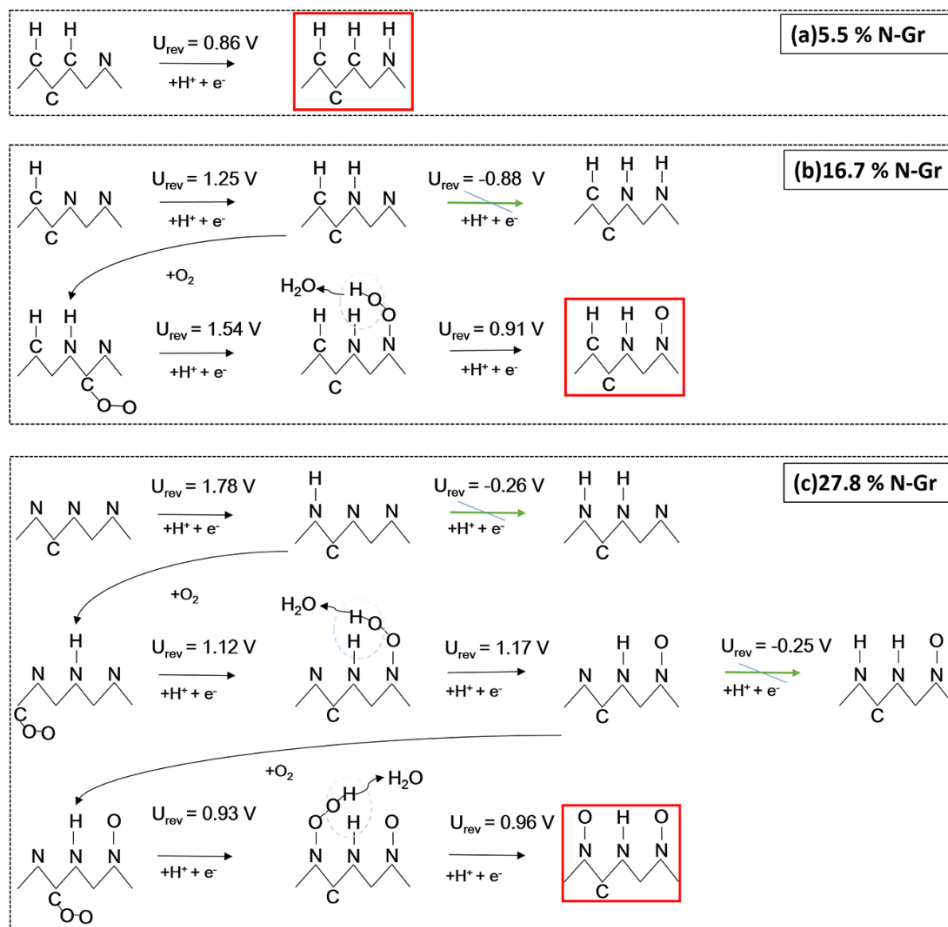


Figure 3. Schematic diagrams explaining the chain of reactions leading to the thermodynamically most stable configurations of edge N-Gr at (a) 5.5 at.% N, (b) 16.7 at.% N and (c) 27.8 at.% N. Each of the model systems was rigorously evaluated for adsorption by solvated protons and O₂ molecules. The reversible potentials for the electrochemical steps were identified using Eq. (2).

The process of H-poisoning becomes more complicated at higher at.% N. As can be seen in the schematic in Fig. 3(b) at 16.7 at.% N, the edge C and its nearest neighbour N atoms can be expected to readily adsorb H atoms below the thermodynamic potential of PEM fuel cells (1.23 V at room temperature), while the other N atom prefers a state without adsorbed H. At the same time adsorption of O₂ at all possible positions was considered, but was found to be thermodynamically feasible only after removal of the dangling bond. In this structure, O₂ was

found to preferentially adsorb on the graphitic C atom near N rather than N. Considering the high reduction potential (1.54 V), which is in fact within the potential window of oxygen gas evolution), however, the reduction of O_2 to OOH^* is very strongly favoured to occur at the edge-located N atom, i.e., the N atom is thermodynamically the active site initiating O_2 reduction reaction. By searching for further thermodynamic reaction processes, we also find that the adsorbed OOH^* can thermodynamically further dissociate into O^* and OH^* by reacting with yet another reduction on the N-Gr surface. Thus, the stable structure of N-Gr with 16.7 at.% N ends up with that marked by the red square at Fig. 3(b).

Such phenomenon of the structural poisoning of dangling bonds by H or O atoms were also found by ab-initio calculations[38] and experimental measurements,[39, 40] which is consistent with the present observations.

Fig. 3(c) shows the processes that leads to the thermodynamically stable configuration of the edge form of N-Gr at 27.8 at.% N, where all edge sites are occupied with N atoms. The thermodynamic path is similar to that of the 16.7 at.% N model: adsorbed O_2 molecules are reduced into OOH^* at the N atom ending up poisoning two of three N atoms. One of the edge N forms chemical bonding with the adsorbed H atom. The reversible potentials are so high and within the windows of water stability regimes that the end-product structure may be quite stable at the PEM fuel cell operational condition as often observed in experiments.[39, 40]

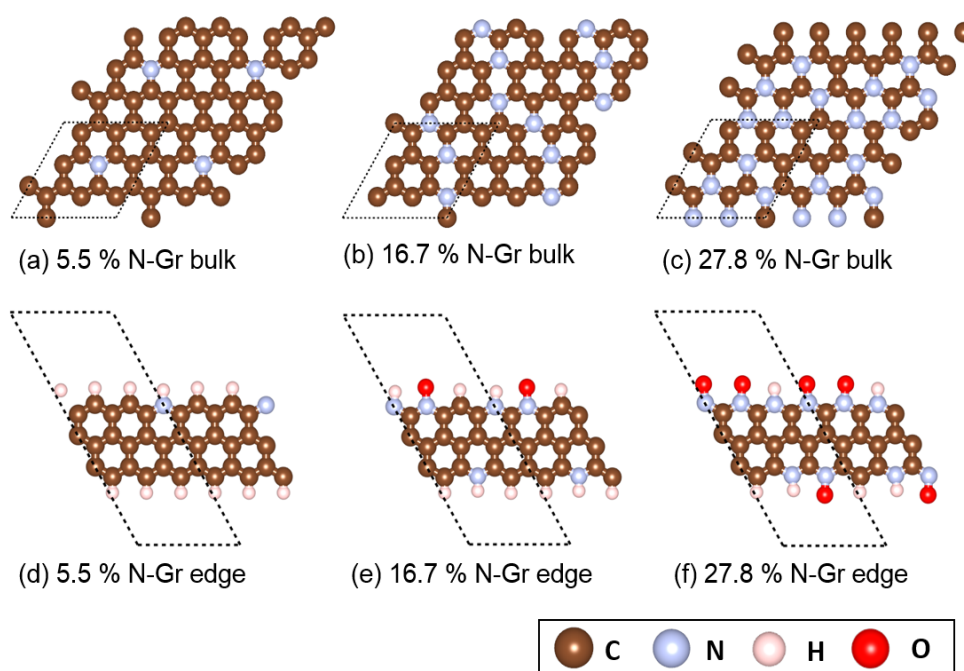


Figure 4. Model bulk and edge N-Gr systems are used in this study to investigate fundamental mechanisms of ORR catalysis. The dashed parallelograms denote the unit cells used in DFT calculations.

The final structures formed after the first ORR processes in edge shapes of N-Gr were illustrated by red-coloured squares in Fig. 3. It is a sort of structural poisoning, since the original structures before the ORR started are not recovered via strong chemical bonding (high reduction potentials) with H or O. One thing worthy of noting is that our results on identifying the initial N-Gr structures formed by the first ORR in Fig. 3 are purely based on the thermodynamic aspects. Kinetic effects, which could require substantial activation energy to accomplish the proposed reaction chain could essentially block a route or may facilitate other mechanistic paths.

Following this detailed analysis, in Fig. 4 we show the bulk (a ~ c) and edge (d ~ f) N-Gr forms with different at.% N that were used to study ORR mechanisms. For the bulk models we adopted the ground state structures as predicted from the energy convex hull shown in Fig. 1, while for edge models the configurations marked in the red boxes in Fig. 3 were adopted.

3. Results and Discussion

3.1. Electronic structures of N-Gr model systems

It has been speculated before that N-Gr reduces O_2 from the gas phase to H_2O via a four-electron pathway, while pristine graphene takes part only in a two-electron process which ends up in peroxide generation.[16, 24] These distinct mechanisms have been attributed to the perturbations in the charge distribution caused by the dopant N atoms.[27] We calculated the spatial variation in the distribution of electronic charges in bulk and edge N-Gr using the Bader Charge analysis[41] as shown in Fig. 5. It can be clearly seen that there is indeed a substantial amount of charge relocation to N from the first nearest neighbour C atoms, leaving the C atoms partially positive, while N is partially negative. This charge distribution is much more favourable for adsorption of any oxygenated species, because the charge distribution leads to a marked decrease in the repulsive electronic force between the lone pair of the oxygen and the 2π electrons the carbon atom.

The amount of charge relocation in the edge form is similar to that in the bulk, but the degree of polarization of nearby C atoms is much stronger in the edge form. The same has been confirmed earlier by Luo et al.,[20] who proposed that the strongly polarized C atom at the first nearest neighbour position to N can mitigate the repulsive interaction between N and O_2 . We stipulate that such an effect results from two factors. First, there are only two C atoms instead of three as found in the bulk model. Second, due to the poisoning of edge N-Gr forms by oxygen and hydrogen as discussed earlier, the electronic charge is redistributed more towards the nitrogen and oxygen atoms because of their higher electronegativity. This polarization of the nearest neighbour C due to the presence of electronegative groups in the nearest and next nearest neighbour positions possibly also helps in inducing the adsorption of O_2 at the C site.

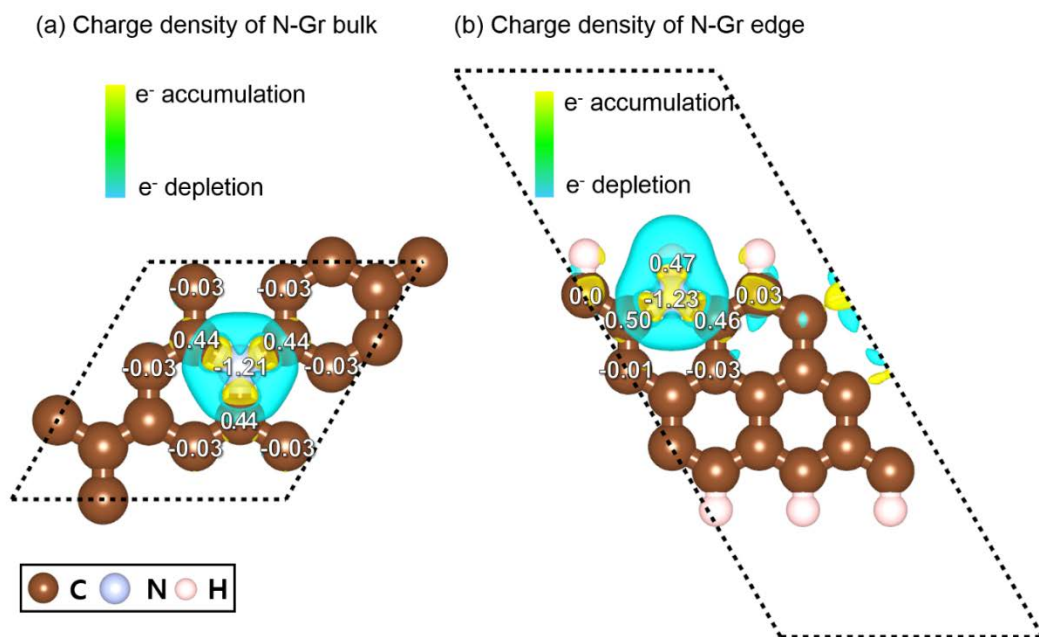


Figure 5. Charge density distribution calculated by Bader's analysis for (a) 5.5 at.% N bulk and in (b) 5.5 at.% N edge N-Gr models.

3.2. Thermodynamic free energy diagram of ORR: Formalism

To understand the fundamental mechanisms of ORR in N-Gr, we calculated thermodynamic free energy diagrams for ORR in each of the model systems, as depicted at Fig. 4, following the procedure as reported in earlier studies.[37, 42] Factors such as electrode potential, pH, and two thermodynamic variables - the dopant concentration and the morphology (either bulk or edge) directly affect the ORR and were considered in this study. In addition to these factors, we also considered the effect of water solvation by H₂O molecules in the model systems until the density reached 1 gcm⁻³. Structures of water were optimized using ab-initio molecular dynamics at T = 300 K over a time span of 2 picoseconds.

The Gibb's free energy of each intermediate can be decomposed into several subcomponents as shown in Eq. (3),

$$\Delta G = \Delta E + \Delta ZPE - T\Delta S + \Delta G_U \quad (3).$$

ΔE is the DFT-calculated total energy of an intermediate, ΔZPE means zero-point energy correction, T is thermodynamic temperature, and ΔS is entropy change, the values of which were borrowed from other sources.[43] We considered the effect of electrode potential (U) as ΔG_U by linearly shifting electronic chemical potential as much as $-nFU$, as stated by Nernst's law (n is the number of electrons involved at each reaction step). We used ΔZPE and entropy corrections as used in earlier studies at $T = 300$ K, $P = 1$ atm and $pH = 0$. [37]

3.3. Gibbs free energy diagrams for ORR: The effect of dopant concentration

In Fig. 6, we show the thermodynamic Gibbs free energy diagrams for ORR for bulk and edged N-Gr as a function of at.% N, but without water solvation. Such an analysis helps in understanding the dependence of ORR on exclusively the binding energy with the catalyst surface. Regardless of composition, our results indicate that the oxygen gas adsorbs associatively on both bulk and edged N-Gr. This is an important distinction to be considered, noting that there is a substantial activation barrier for a pure Gr to adsorb oxygen gas, which is eventually reduced into peroxide at PEM fuel cell operational conditions. We propose that this change in activity can be explained as the result of the partial electronic polarization at C atoms neighbouring the dopant N atoms as described in the section of Poisoning of dangling bonds in edge N-Gr, which enables N-Gr to attractively interact with oxygen by lowering the activation barrier for chemical adsorption.

The free energy diagrams in Fig. 6 show that the ORR mechanisms in bulk and edged N-Gr are sensitive to dopant concentration and morphology of N-Gr. At 5.5 at.% N, the ORR mechanisms are associative in the N-Gr, but dissociative in all other bulk N-Gr models. This is because the charge deficiency at the C atom also increases as at.% of doped N increases, thus making its bond with the OOH^* intermediate much stronger, eventually resulting in the dissociation of OOH^* into O^* and OH^* . We find that onset potential for the electrochemical reduction of O_2 to OOH^* at 5.5 at.% N is 0.55 V, at which the free energies of both O_2 and OOH^* are equal (i.e. in equilibrium). Over all, the reduction step of O_2 into OOH^* in 5.5 at.% N doped bulk N-Gr is likely to have thermodynamically the lowest driving force. While the effect of the doping level on the free energy of OH^* is marginal, its impact is crucial on O^* . This can be clearly observed in the last two reduction steps in Fig. 6(a). As

the at.% N increases, the binding energy of O* increases and that of OH* remains largely unaffected. It shifts thermodynamic tailback to the electrochemical reduction of O* to OH* as at.% N increases. In fact, O* is found to be so strongly stabilized in the 27.8 at.% N model, that there is no ORR activity. Remarkably, it is these different dependencies of O* and OH* on dopant concentration that eventually lead to substantial amounts of overpotential for ORR. The effect of N doping on the onset potentials of ORR in bulk N-Gr is negative: 0.55 V at 5.5 at.% N to 0 V at 27.8 at.% N doped bulk Gr.

ORR mechanisms without solvation in all edged N-Gr are found to be associative, and the free energy for the electrochemical reduction of O₂ to OOH* is uphill in the entire potential range of 0 and 1.23 V. Unfortunately, this result bears similarity with ORR in a pristine graphene, which gives rise to peroxide via the two-electron process. Unlike in bulk N-Gr, the effect of at.% N on ORR efficiency in edged N-Gr is small. Although the Gibbs free energies of intermediates are stabilized as at.% N increases (as shown Fig. 6(a)), the large overpotential of the first ORR step still remains.

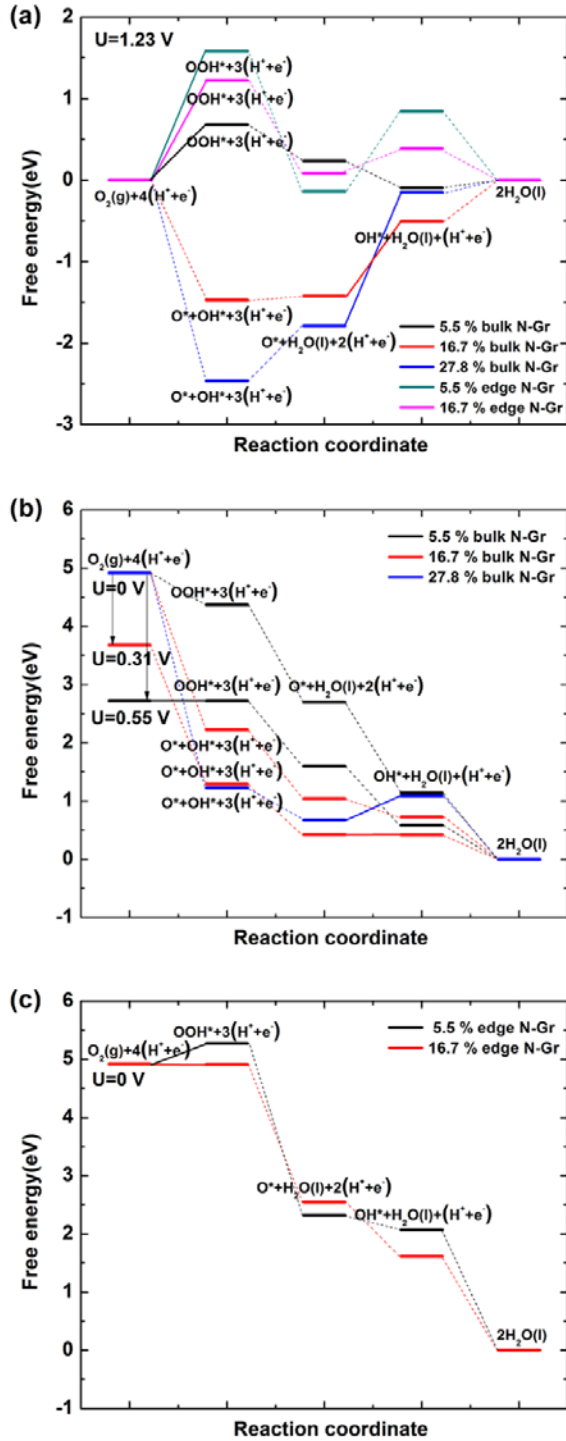


Figure 6. (a) Free energy diagrams of ORR on edge and bulk N-Gr models at potential $U = 1.23$ V. Free energy diagrams of ORR at thermodynamic onset potentials on bulk N-Gr models (b) and edge N-Gr models (c). Here, the effect of water solvation was not considered, and the solid lines represent potential determining step.

Interestingly, the N-Gr edged form with 27.8 at.% N shows a completely different ORR mechanism than the other models. The ORR pathway for 27.8 at.% N edged N-Gr, as illustrated in Fig. 7, shows that even though the edge N atoms are active toward reducing O_2 into OOH^* , the chemically poisoned structure energetically forces oxygen gas to adsorb on the C connecting the N atoms, at which it is reduced to OOH^* at relatively low potentials below 0.24 V. Further, it was found that the N-Gr framework could be broken during a simultaneous detachment of the chemical bond between C and N and the protonation of OOH^* at C resulting into formation of a H_2O molecule. The calculated reversible potential (3.10 V) indicates a high thermodynamic driving force for the reaction at PEM fuel cell operational condition. Kim et al.[25] found the same behaviour. The thermodynamic calculations presented here for further reactions suggest that the broken framework can be eventually restored through a series of chain reactions. The potential window of the reversible reactions is so wide (0.24 ~ 3.10 V) that the breaking and restoring mechanism of the N-Gr framework is of importance as the operational potential of PEM fuel cell is repetitively cycled within this potential range. Our results imply that the structural integrity of a 27.8 at.% doped N-Gr, however, should be very vulnerable to serious degradation, once thermodynamic conditions vary or any kinetic factor becomes important in the ORR process.

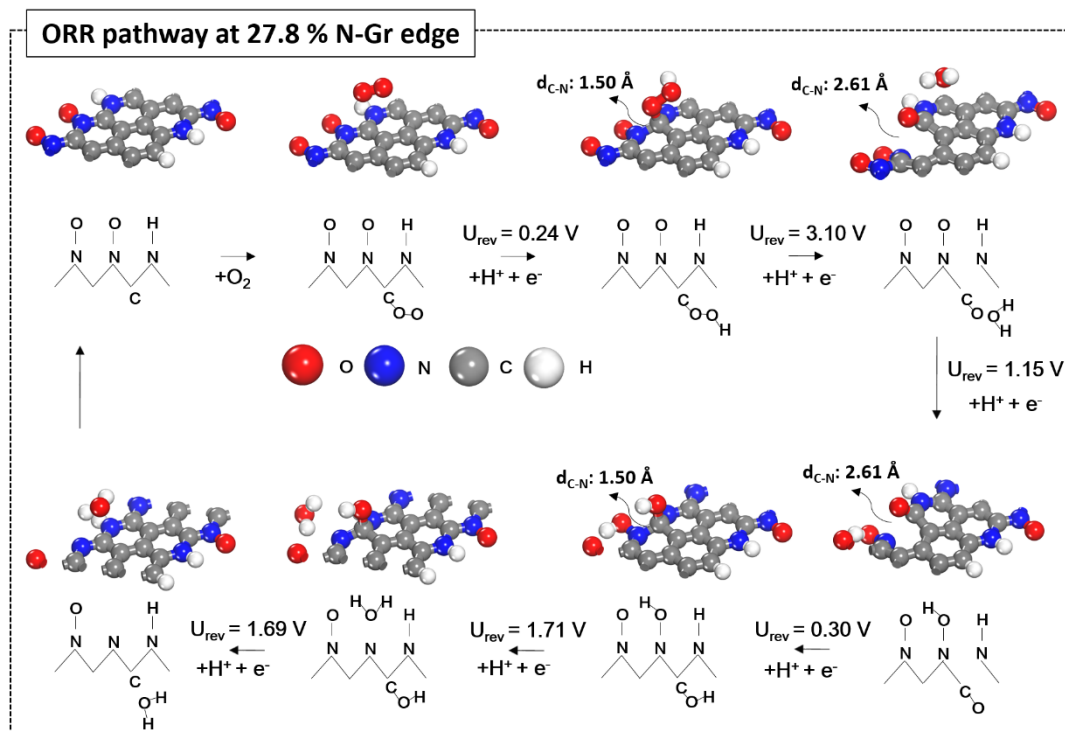


Figure 7. A proposed ORR pathway for the edged form of N-Gr with 27.8 at.% N-doping level. Detailed catalysis cycle for ORR of the edged form of N-Gr was illustrated via a series of electrochemical reaction steps.

To summarize the results for the bulk N-Gr without water solvation, the catalytic efficiency towards ORR decreases as the at.% N increases. The mechanism is dictated mostly by the stabilization of adsorbed O^* by the doped N, thus making the reduction of O^* into OH^* the thermodynamically most difficult step. In other words, the potential energy surface of bulk N-Gr manifests itself in a shape considerably biased towards O^* but not OH^* or OOH^* . In the edged form of N-Gr, thermodynamic efficiency of ORR is found to be worse than in the bulk form, even though the doped N almost stabilizes all of the oxygen containing chemical species. The higher the N doping level is, the worse the ORR activity. This analysis of ORR mechanisms without the solvation effect of water sheds light on the ways the mechanisms could be influenced by the binding energy of the intermediates.

3.4. Thermodynamic free energy diagram of ORR: Effect of water solvation

We calculated the thermodynamic Gibbs free energy diagrams of bulk and edged N-Gr models exposed to a water environment. We placed 16 and 39 H₂O molecules in bulk and edged form of N-Gr model systems, respectively, to make the water density 1 gcm⁻³ in each. The water structure was then optimized using ab-initio molecular dynamics for 2 picoseconds at T = 300 K.

Fig. 8 illustrates the calculated thermodynamic free energy diagrams of ORR in the bulk and edged N-Gr models under water solvation. In case of bulk N-Gr, although the Gibbs free energies of ORR intermediates shift to more negative values (implying higher stabilization), the overall trends largely remain the same as those without water solvation. The onset potential for ORR at 5.5 at.% N in the bulk form increases from 0.55 V to 0.79 V after inclusion of a water environment (as shown in Fig. 6 (b) and 8 (b)), and the increased onset potential is comparable to it on Pt catalyst.[44] We propose that such an effect arises as a result of the thermodynamic stabilization of adsorbed OOH* by the surrounding H₂O molecules, which lowers the onset potential for reduction of O₂. This result is in good agreement with experiments.[17-19, 21] In total, the effect of dopant N atoms stabilizing adsorbed oxygen atoms is dominant over the impact of water solvation, because the effect of solvation due to water molecules in bulk N-Gr model is similar across all intermediates.

In the edge N-Gr model, although the adsorbed OOH* species becomes slightly stable at 16.7 at.% N doping levels (as shown in Fig. 6(a) and 8(a), the first reduction step of O₂ to OOH* with water molecules is still found to face a large overpotential for the first reaction step. Unfortunately, the onset potentials for ORR at the edged form of N-Gr are almost zero with water. Although the presence of dopant and water solvation lead to possible stabilization of the intermediates, the weak adsorption of OOH species at edged N-Gr leads to a very large overpotential. This seems to suggest that ORR will not be feasible on the edge forms of doped N-Gr. These findings agree well with recent experiments.[20, 21, 45, 46]

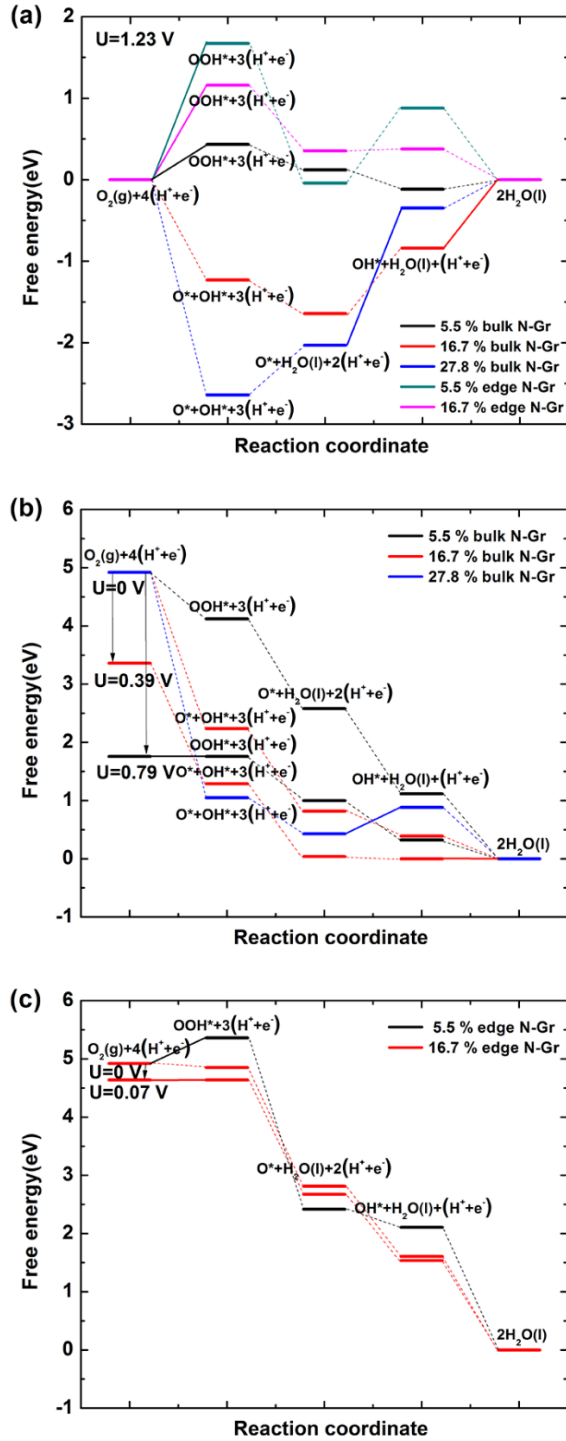


Figure 8. (a) Free energy diagrams of ORR on edge and bulk N-Gr models at potential $U = 1.23$ V. Free energy diagrams of ORR at thermodynamic onset potentials on bulk N-Gr models (b) and edge N-Gr models (c). Here, the effect of water solvation was considered, and the solid lines represent potential determining step.

4. Conclusion

Using first principles DFT calculations, we analysed catalytic activity of N-Gr toward ORR, which is found to be significantly influenced by atomistic morphology and concentration of dopant N atoms. A rigorous process to identify the thermodynamically most stable structures was employed for bulk and edge shapes of N-Gr, after which poisoning of the edged form N-Gr under a reducing environment was also considered in detail. Without the effect of aqueous solvation, the catalytic efficiency towards ORR is found to be mostly controlled by the strong chemical stabilization of adsorbed O* in bulk N-Gr due to the dopant N, thus making the reduction of O* into OH* thermodynamically the most difficult step. The phenomenon is more conspicuous in edged forms of N-Gr leading to even lower ORR onset potentials than in bulk N-Gr. The effect of water solvation on ORR activity is stronger at dilute N doping levels and diminishes as the N concentration increases. Thus, the solvation by water molecules contributes only marginally to controlling ORR activity of N-Gr compared with the effect of N-doping. Based on these findings, we propose that bulk form N-Gr catalysts with dilute N concentration are more optimized towards ORR catalysis. The extensive analysis of finding stable structure and determining ORR mechanism present in this study is useful for rational design of promising non-precious catalysts, and can also be applied to other areas where one hopes to upgrade the parent material properties by a heteroatom doping.

References

- [1] Studt, F., Sharafutdinov, I., Abild-Pedersen, F., Elkjær, C. F., Hummelshøj, J. S., Dahl, S., Chorkendorff, I., Nørskov, J. K., "Discovery of a Ni-Ga catalyst for carbon dioxide reduction to methanol." *Nature chemistry*, **6**, 2014, pp. 320-324.
- [2] Wang, X., Maeda, K., Thomas, A., Takanabe, K., Xin, G., Carlsson, J. M., Domen, K., Antonietti, M., "A metal-free polymeric photocatalyst for hydrogen production from water under visible light." *Nature Materials*, **8**, 2008, pp. 76-80.
- [3] Yu, L., Pan, X., Cao, X., Hu, P., Bao, X., "Oxygen reduction reaction mechanism on nitrogen-doped graphene: a density functional theory study." *Journal of Catalysis*, **282**, 2011, pp. 183-190.
- [4] Bruce, P. G., Freunberger, S. A., Hardwick, L. J., Tarascon, J.-M., "Li-O₂ and Li-S batteries with high energy storage." *Nature materials*, **11**, 2012, pp. 19-29.
- [5] Peng, Z., Freunberger, S. A., Chen, Y., Bruce, P. G., "A reversible and higher-rate Li-O₂ battery." *Science*, **337**, 2012, pp. 563-566.
- [6] Debe, M. K., "Electrocatalyst approaches and challenges for automotive fuel cells." *Nature*, **486**, 2012, pp. 43-51.
- [7] Steele, B. C., Heinzel, A., "Materials for fuel-cell technologies." *Nature*, **414**, 2001, pp. 345-352.
- [8] Noh, S. H., Seo, M. H., Seo, J. K., Fischer, P., Han, B., "First principles computational study on the electrochemical stability of Pt-Co nanocatalysts." *Nanoscale*, **5**, 2013, pp. 8625-8633.
- [9] Grätzel, M., "Photoelectrochemical cells." *Nature*, **414**, 2001, pp. 338-344.
- [10] Boukai, A. I., Bunimovich, Y., Tahir-Kheli, J., Yu, J.-K., Goddard Iii, W. A., Heath, J. R., "Silicon nanowires as efficient thermoelectric materials." *Nature*, **451**, 2008, pp. 168-171.
- [11] Wang, X., Li, X., Zhang, L., Yoon, Y., Weber, P. K., Wang, H., Guo, J., Dai, H., "N-doping of graphene through electrothermal reactions with ammonia." *Science*, **324**, 2009, pp. 768-771.
- [12] Norris, D. J., Efros, A. L., Erwin, S. C., "Doped nanocrystals." *Science*, **319**, 2008, pp. 1776-1779.
- [13] Zhao, L., He, R., Rim, K. T., Schiros, T., Kim, K. S., Zhou, H., Gutiérrez, C., Chockalingam, S., Arguello, C. J., Pálová, L., "Visualizing individual nitrogen dopants in monolayer graphene." *Science*, **333**, 2011,

pp. 999-1003.

- [14] Rabis, A., Rodriguez, P., Schmidt, T. J., "Electrocatalysis for polymer electrolyte fuel cells: recent achievements and future challenges." *Acs Catalysis*, **2**, 2012, pp. 864-890.
- [15] Wang, H., Maiyalagan, T., Wang, X., "Review on recent progress in nitrogen-doped graphene: synthesis, characterization, and its potential applications." *Acs Catalysis*, **2**, 2012, pp. 781-794.
- [16] Qu, L., Liu, Y., Baek, J.-B., Dai, L., "Nitrogen-doped graphene as efficient metal-free electrocatalyst for oxygen reduction in fuel cells." *ACS nano*, **4**, 2010, pp. 1321-1326.
- [17] Geng, D., Chen, Y., Chen, Y., Li, Y., Li, R., Sun, X., Ye, S., Knights, S., "High oxygen-reduction activity and durability of nitrogen-doped graphene." *Energy Environ. Sci.*, **4**, 2011, pp. 760-764.
- [18] Choi, C. H., Chung, M. W., Kwon, H. C., Park, S. H., Woo, S. I., "B, N-and P, N-doped graphene as highly active catalysts for oxygen reduction reactions in acidic media." *Journal of Materials Chemistry A*, **1**, 2013, pp. 3694-3699.
- [19] Choi, C. H., Park, S. H., Woo, S. I., "Binary and ternary doping of nitrogen, boron, and phosphorus into carbon for enhancing electrochemical oxygen reduction activity." *ACS nano*, **6**, 2012, pp. 7084-7091.
- [20] Luo, Z., Lim, S., Tian, Z., Shang, J., Lai, L., MacDonald, B., Fu, C., Shen, Z., Yu, T., Lin, J., "Pyridinic N doped graphene: synthesis, electronic structure, and electrocatalytic property." *Journal of Materials Chemistry*, **21**, 2011, pp. 8038-8044.
- [21] Zhang, Y., Ge, J., Wang, L., Wang, D., Ding, F., Tao, X., Chen, W., "Manageable N-doped graphene for high performance oxygen reduction reaction." *Scientific reports*, **3**, 2013, pp. 2771.
- [22] Parvez, K., Yang, S., Hernandez, Y., Winter, A., Turchanin, A., Feng, X., Müllen, K., "Nitrogen-doped graphene and its iron-based composite as efficient electrocatalysts for oxygen reduction reaction." *Acs Nano*, **6**, 2012, pp. 9541-9550.
- [23] Boukhvalov, D. W., Son, Y.-W., "Oxygen reduction reactions on pure and nitrogen-doped graphene: a first-principles modeling." *Nanoscale*, **4**, 2012, pp. 417-420.
- [24] Jiao, Y., Zheng, Y., Jaroniec, M., Qiao, S. Z., "Origin of the electrocatalytic oxygen reduction activity of graphene-based catalysts: a roadmap to achieve the best performance." *Journal of the American Chemical Society*, **136**, 2014, pp. 4394-4403.
- [25] Kim, H., Lee, K., Woo, S. I., Jung, Y., "On the mechanism of enhanced oxygen reduction reaction in

- nitrogen-doped graphene nanoribbons." *Physical Chemistry Chemical Physics*, **13**, 2011, pp. 17505-17510.
- [26] Okamoto, Y., "First-principles molecular dynamics simulation of O₂ reduction on nitrogen-doped carbon." *Applied Surface Science*, **256**, 2009, pp. 335-341.
- [27] Zhang, L., Xia, Z., "Mechanisms of oxygen reduction reaction on nitrogen-doped graphene for fuel cells." *The Journal of Physical Chemistry C*, **115**, 2011, pp. 11170-11176.
- [28] Fan, X., Zheng, W., Kuo, J.-L., "Oxygen reduction reaction on active sites of heteroatom-doped graphene." *RSC Advances*, **3**, 2013, pp. 5498-5505.
- [29] Kresse, G., Furthmüller, J., "Efficiency of ab-initio total energy calculations for metals and semiconductors using a plane-wave basis set." *Computational Materials Science*, **6**, 1996, pp. 15-50.
- [30] Kresse, G., Hafner, J., "Ab initio molecular dynamics for liquid metals." *Physical Review B*, **47**, 1993, pp. 558.
- [31] Blöchl, P. E., "Projector augmented-wave method." *Physical Review B*, **50**, 1994, pp. 17953.
- [32] Perdew, J. P., Burke, K., Ernzerhof, M., "Generalized gradient approximation made simple." *Physical review letters*, **77**, pp. 1996, 3865.
- [33] Grimme, S., "Semiempirical GGA-type density functional constructed with a long-range dispersion correction." *Journal of computational chemistry*, **27**, 2006, pp. 1787-1799.
- [34] Van der Ven, A. A. F., "First principles investigation of the thermodynamic and kinetic properties of lithium transition metal oxides." *Ph.D. thesis*, Massachusetts Institute of Technology, 2000, 164.
- [35] Liu, A. Y., Wentzcovitch, R. M., "Stability of carbon nitride solids." *Physical Review B*, **50**, 1994, pp. 10362.
- [36] Souto, S., Pickholz, M., Dos Santos, M., Alvarez, F., "Electronic structure of nitrogen-carbon alloys (a-CN_x) determined by photoelectron spectroscopy." *Physical Review B*, **57**, 1998, pp. 2536.
- [37] Nørskov, J. K., Rossmeisl, J., Logadottir, A., Lindqvist, L., Kitchin, J. R., Bligaard, T., Jonsson, H., "Origin of the overpotential for oxygen reduction at a fuel-cell cathode." *The Journal of Physical Chemistry B*, **108**, 2004, pp. 17886-17892.
- [38] Kurak, K. A., Anderson, A. B., "Nitrogen-treated graphite and oxygen electroreduction on pyridinic edge sites." *The Journal of Physical Chemistry C*, **113**, 2009, pp. 6730-6734.

- [39] Geng, D., Yang, S., Zhang, Y., Yang, J., Liu, J., Li, R., Sham, T.-K., Sun, X., Ye, S., Knights, S., "Nitrogen doping effects on the structure of graphene." *Applied Surface Science*, **257**, 2011, pp. 9193-9198.
- [40] Wang, Y., Shao, Y., Matson, D. W., Li, J., Lin, Y., "Nitrogen-doped graphene and its application in electrochemical biosensing." *Acs Nano*, **4**, 2010, pp. 1790-1798.
- [41] Tang, W., Sanville, E., Henkelman, G., "A grid-based Bader analysis algorithm without lattice bias." *Journal of Physics: Condensed Matter*, **21**, 2009, pp. 084204.
- [42] Han, B., Viswanathan, V., Pitsch, H., "First-principles based analysis of the electrocatalytic activity of the unreconstructed pt (100) surface for oxygen reduction reaction." *The Journal of Physical Chemistry C*, **116**, 2012, pp. 6174-6183.
- [43] Atkins, P., de Paula, J., *Physical Chemistry Volume 1: Thermodynamics and Kinetics*, Macmillan Higher Education, 2009.
- [44] Hansen, H. A., Rossmeisl, J., Nørskov, J. K., "Surface Pourbaix diagrams and oxygen reduction activity of Pt, Ag and Ni (111) surfaces studied by DFT." *Physical Chemistry Chemical Physics*, **10**, 2008, pp. 3722-3730.
- [45] Sidik, R. A., Anderson, A. B., Subramanian, N. P., Kumaraguru, S. P., Popov, B. N., "O₂ reduction on graphite and nitrogen-doped graphite: experiment and theory." *The Journal of Physical Chemistry B*, **110**, 2006, pp. 1787-1793.
- [46] Shao, Y., Sui, J., Yin, G., Gao, Y., "Nitrogen-doped carbon nanostructures and their composites as catalytic materials for proton exchange membrane fuel cell." *Applied Catalysis B: Environmental*, **79**, 2008, pp. 89-99.

국문요약

제 1 원리 전산을 이용하여 모폴로지, 도핑농도, 용매가 그래핀에서 산소환원반응에 미치는 영향 분석

연료전지는 에너지 생산문제를 해결할 수 있는 유망한 신 재생에너지원으로 조명되고 있지만, 비싼 백금촉매가격 및 상용화에는 부족한 내구성과 촉매활성 문제로 어려움을 겪고 있다. 최근, 백금촉매를 대체할 수 있는 비 백금 촉매를 개발하기 위한 연구가 진행되고 있다. 비 백금촉매 중에서 질소도핑 그래핀(N-Gr)은 백금촉매와 비슷한 산소환원반응(ORR) 촉매활성이 보고되었다. 그러나, 산소환원반응에 기여하는 N-Gr의 구체적인 구조는 밝혀지지 않았고 N-Gr에서의 산소환원반응 메커니즘에 대해서도 많은 연구가 필요하다.

본 논문은 제 1 원리 전산을 이용하여 N-Gr의 구조와 농도에 따른 안정한 구조들을 찾고, 산소환원반응에 대한 촉매 거동을 원자 단위 수준에서 밝히고자 하였다. 나노 리본 및 벌크 형태의 그래핀에 질소의 농도함수로서 도핑된 약 1000 개의 N-Gr 구조들에 대한 에너지를 계산하였고 에너지 컨벡스 힐 방법을 사용하여 열역학적으로 안정한 N-Gr 구조들을 확인하였다. 질소농도가 27 at.% 이상이 되면 그래핀의 구조가 붕괴되는 것을 확인하였다. 이러한 결과들은 실험적인 결과와 잘 일치한다.

질소도핑 그래핀에서 산소환원반응에 대한 이해를 얻기 위해서 반응 중간 생성물의 에너지를 계산하였고, 열역학적인 이론을 적용하여 촉매반응에 대한 활성과 반응 메커니즘을 확인하였다. 본 연구에서는 질소농도가 낮은 벌크 형태의 N-Gr 구조에서 가장 높은 촉매활성을 보인다는 것을 확인하였다. 또한, 물이 있는 환경이 촉매활성에 미치는 영향을 확인하였다. 물은 반응 중간생성물들의 에너지를 안정화시키는 역할을 하며, 이러한 효과는 백금과 비슷한 산소환원반응 촉매활성을 가질 수 있는 요인임을 밝혔다.

핵심어: 제 1 원리, 신 재생에너지, 그래핀, 촉매, 산소환원반응

Acknowledgement

먼저, 석사 학위 과정 2 년 동안 많은 조언을 해주시고 좋은 연구자가 될 수 있도록 지도를 해주신 한병찬 교수님께 감사의 말씀을 드립니다. 논문이 완성되기까지 유익한 조언을 해주신 Sangaraju Shanmugam 교수님, 윤영기 박사님께도 감사의 인사를 드립니다.

2 년이라는 석사 학위 과정 동안, AICODES 멤버들 덕분에 학위과정을 잘 마칠 수 있었던 것 같습니다. 석사과정 초기에 연구하는데 많은 조언을 해주시고 흥미를 갖게 도와주셨던 서민호 박사님, 동기로 동고동락을 같이했던 주승이, 종교인으로서 배울 점이 많았던 상흠이형, 항상 연구에 흥미를 갖고 연구를 즐기시는 승효형, 2 년 동안 항상 든든한 버팀목이 되어주셨던 준희형, 고생을 많이 했던 혜진이누나, 수연이, 컴퓨터를 좋아하는 영록이형, 그리고 좋은 기억을 함께한 AICODES를 거쳐갔던 많은 분들에게 감사합니다.

AICODES 멤버는 아니지만, 2 년 동안 같이 생활하면서 많은 조언과 도움을 주었던 기돈이형 및 다른 선배님들에게도 감사하다는 말을 하고 싶습니다.

마지막으로, 항상 제가 가고자 하는 길을 조용히 지지해 주시고 함께해 주신 부모님과 친구들에게 감사합니다. 모두 사랑합니다.

Curriculum Vitae

Dohyun Kwak

Department of Energy Systems Engineering
DGIST, Daegu

EDUCATION

- B.S. in Department of mechanical Engineering, Cunnam National University, Feb 2013

RESEARCH INTERESTS

- Ab-initio computational study of ORR mechanism on graphene based materials
- First principles computational design of high-functional renewable energy materials for fuel cells
- Ab-Initio and multi-scale computational design of pyro-process of spent nuclear fuels using molten salt electrolytes

PUBLICATIONS

- D.H. Kwak, A. Khetan, H. Pitsch, S. H. Noh, B. C. Han, First Principles Study of Morphology, Doping Level and Water Solvation Effects on Catalytic Mechanism of a Graphene Towards Oxygen Reduction Reaction, *ChemCatChem*, 6(9), 2662-2670 (2014)
- D. H. Kwak, S. H. Noh, B. C. Han, Multi-scale Computational Study of the Molten-salt Based Recycling of Spent Nuclear Fuels, *International Journal of Energy Research (top journal of Nuclear Sci. and Eng.)*, 38(15), 1987-1993 (2014)
- S. H. Noh, D. H. Kwak, M. H. Seo, T. Ohsaka and B. C. Han, First principles study of oxygen reduction reaction mechanisms on N-doped graphene with a transition metal support, *Electrochimica Acta (Special Edition)*, 140, 225-231 (2014)
- S.H. Noh, D. H. Kwak, J. S. Lee, J. H. Kang, B. C. Han, First Principles Calculations on Thermodynamic Properties of Transuranium in a Molten Salt Medium, *Journal of the Korean Physical Society*, 64 (6), 806-812 (2014)
- S. H. Noh, J. H. Kang, D. H. Kwak, P. Fischer, B. C. Han, First principles thermodynamic studies for recycling spent nuclear fuels using electrorefining with a molten salt electrolyte, *Energy*, 68, 751-755 (2014)
- G. J. Go, D. H. Kwak, L. Piao, H. C. Choi, S. M. Jeong, C. Lee, B. J. Park, S. Y. Ko, J. O. Park, S. H. Park, Manipulation of micro-particles using a magnetically actuated microrobot, *Mechatronics*, 23, 1037-1043 (2013)

CONFERENCE PRESENTATIONS

- Dohyun Kwak, and Byungchan Han, “First Principles Computational Studies of Catalytic Activity and Electrochemical Stability of Pt-Co alloy Nanoparticles”, The 2nd International Conference on Advanced Electromaterials, Nov 2013 (poster presentation : Best Poster Award)
- Dohyun Kwak, and Byungchan Han, “First Principles Studies on ORR Mechanism of Doped Graphene and Metal-N Doped Graphene”, ASIAN-16, Oct 2013 (poster presentation)
- Dohyun Kwak, and Byungchan Han, “Understanding of Catalytic Mechanisms Towards Oxygen Reduction Reaction in Nitrogen-doped Graphenes: First Principles Study”, 1st DGIST-LBNL Future Energy Materials Workshop, May 2014 (poster presentation: Poster Award)
- Dohyun Kwak, and Byungchan Han, “Understanding of Catalytic Mechanisms Towards Oxygen Reduction Reaction in Nitrogen-doped Graphenes: First Principles Study” 제 10 회 고등과학원 전자구조계산학회, June 2014
- Dohyun Kwak, and Byungchan Han, “Understanding of Catalytic Mechanisms Towards Oxygen Reduction Reaction in Nitrogen-doped Graphenes: First Principles Study”, International Conference on Microelectronics and Plasma Technology, June 2014 (poster presentation)
- Dohyun Kwak, Abhishek Khetan, Heinz Pitsch, Seunghyo Noh, Byungchan Han, “Understanding of catalytic mechanisms towards oxygen reduction reaction in heteroatom-doped graphenes: first principles study” '2nd DGIST-WASEDA Workshop on Electrochemistry, Aug 2014 (poster presentation)
- Dohyun Kwak, and Byungchan Han, “Understanding of Catalytic Mechanisms Towards Oxygen Reduction Reaction in Nitrogen-doped Graphenes: First Principles Study”, Special Doctoral Program for Green Energy Conversion Science and Technology, Aug 2014 (poster presentation)

TEACHING EXPERIENCE

Teaching Assistant, Department of Energy Systems Engineering, DGIST

- ES601: Thermodynamics (2014)